Journal of Inorganic and Organometallic Polymers and Materials
https://doi.org/10.1007/s10904-019-01430-7

Synthesis, Doping and Characterization of new Molecular Semiconductors Containing (2E, 4Z)-5, 7-diphenylhepta-2, 4-dien-6-ynoic acids

R. Ballinas-Indili[1] · M. E. Sánchez-Vergara[2] · Rubén A. Toscano[1] · C. Álvarez-Toledano[1]

Received: 9 October 2019 / Revised: 17 December 2019 / Accepted: 23 December 2019

Abstract
This work refers to the synthesis and characterization of new (2E, 4Z)-5, 7-diphenylhepta-2, 4-dien-6-ynoic acids. We describe the nucleophilic addition of bis(trimethylsylil)ketene acetals (TMS) to aryl ynones substituted by halogen groups activated by boron trifluoride diethyl etherate ($BF_3.Et_2O$) for the stereoselective synthesis of dienynoic acid. The molecular materials were structurally characterized by IR spectroscopy, NMR spectroscopy and X-ray diffraction. After the characterization the synthesized acids were doped with indium(III) phthalocyanine chloride (In(III)PcCl) in order to generate a organic semiconductor that was characterized by UV–Vis spectroscopy to subsequently obtain their optical bandgap (Eg) values. The Eg value was compared to that obtained for the pure state dienynoic acids in order to evaluate the doping effect with the In(III)PcCl. The Eg diminished from values near 2.6 eV obtained for pure compounds to values around 1.4 eV for the same compounds, but now with doping. With the molecular semiconductors obtained were manufactured structures of disperse heterojunction which later were evaluated in their electric behavior. A behaviour ohmic at low voltages and Space Charge Limited Current (SCLC) at higher voltages was observe from the study *J(V)* carried out.

Keywords Dienynoic acid · Molecular semiconductor · Optical bandgap · Electrical properties

1 Introduction

Most of the solid-state electronics device that are currently on the market are manufactured with semiconductor materials; however, the high cost of germanium, the technological limitations associated with the use of silicon, and the successful development in the organic semiconductor materials have led to the development of organic electronics. Examples include the development of the first organic transistor (OFET) based on a semiconducting film of polythiophene [1] and the first hybrid solar cells made from conjugated polymers [2–4]. Organic semiconductors can be classified in different categories: one integrates conjugated polymers, while in the second category we find semiconductors based on small molecules, also called molecular materials. These organic semiconductors are especially promising in the field of organic electronics [5–7] since they present some advantages over silicon technologies, such as their relatively simple processability, low cost production, large coverage area, and flexibility. The most important aspects to consider during the synthesis and preparation of the organic semiconductor were the generation of structures with high π-conjugation, molecular packing with strong overlapping. In recent decades, interest has been devoted to the development of new stereo-selective routes to conjugated polyenes and polyenyne systems [8], a class of compounds which includes natural products such leukotrine B4, a regulator of immune response and retinaldehyde, a chemical compounds involved in animal vision [9, 10]. These molecules are polyunsaturated organic compounds that interacted in conjugation process, resulting in some unusual optical and electrical properties [11–13]. In this paper we presented the direct formation of stereo-defined dienes functionalised

✉ M. E. Sánchez-Vergara
elena.sanchez@anahuac.mx

✉ C. Álvarez-Toledano
cecilio@unam.mx

[1] Instituto de Química, Universidad Nacional Autónoma de México, Circuito Exterior Ciudad Universitaria, C. P. 04510 Ciudad de México, México

[2] Universidad Anáhuac México, Estado de México, Avenida Universidad Anáhuac 46, Col. Lomas Anáhuac, C.P. 52786 Huixquilucan, México

Published online: 01 January 2020

under mild conditions and with complete atom economy [14–16]. The essential synthetic problem has been to prepare the functionalized diene system in a highly stereo-selective manner, and a wide variety of synthetic approaches have been used. 2,4-Dienoic acids and their derivatives are useful starting materials for the preparation of available natural products with fixed configurations *E,E*-, *E,Z*-, and Z,Z-isomers. The conjugated polyenes have been synthesized by the Horner–Wadsworth–Emmons reaction from stabilized phophonate carbanions and several coupling reactions, such as the Suzuki approach, McMurry coupling, and the Stille approach [17–25]. Abarbri et al. reported obtaining dienynoic acids under Sonogashira conditions from alkynes and iodoalkadienoic acid using dichloro*bis*(triphenylphosphine) palladium (II) and copper (I) iodide as catalysts under mild experimental conditions [26]. An efficient procedure has been described for the synthesis of captodative dienyne acids by reaction of the corresponding Fisher alkynil carbene complexes with 2-(trimethylsiloxi) furan in a one-pot process [27].

Here, we describe the stereoselective synthesis of (2E, 4Z) dienynoic acids based on the nucleophilic addition of *bis*(TMS)ketene acetals to aryl ynones substituted by halogen groups using an efficient and simple procedure (Fig. 1). It is important to note that the diene products were obtained in geometrically pure (*E,Z,*)-configurations, highlighting the mildness of the reaction conditions and the simplicity of the procedure. A strategy to increase their charge mobility is to introduce electro-acceptant groups, where hydrogen atoms are replaced by fluorine atoms [28]. Marks et al. synthesized type-*n* semiconductors, making functional thiophene oligomers with perfluorinated substituents [29–32], while Bao et al. synthesized derivatives of imides with different halogens as substituents in the nucleus of perylene and different fluorinated substituents in imidic positions [33, 34]. In the current study, the introduction of halogens in the structure of the (2E, 4Z) dienynoic acids it was carried out in order to enhance their behaviour as *n*-type semiconductors. The objective of the present study was centred in two parts, (i) the synthesis and characterization of conjugated molecular materials based on (2E, 4Z)-5, 7-diphenylhepta-2, 4-dien-6-ynoic acids. To ensure *n*-type semiconductor behaviour, the synthesis of (2E, 4Z) dienynoic acids is based on the nucleophilic addition of *bis*(TMS)ketene acetals to aryl ynones substituted by electro-acceptor groups (F^-, Cl^-, Br^-). (ii) These (2E, 4Z)-5, 7-diphenylhepta-2, 4-dien-6-ynoic acids were doped with the *p*-type semiconductor indium(III) phthalocyanine chloride (In(III)PcCl) and the molecular semiconductors were optically characterized. The diamagnetic indium(III) metal cation was selected in this study as central metal in the phthalocyanine cavity for enhance the optical properties [35–37]. Aditionally the mono-axially chloro substituted indium(III)phthalocyanine is especially known as a promising material for nonlinear optic devices [38–40].

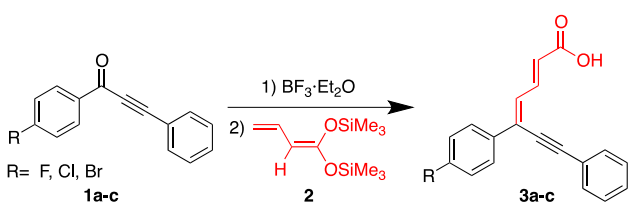

Fig. 1 Synthesis of (2E, 4Z) dienynoic acids

2 Experimental Section

We started the study with the reaction of 1-(4-fluorophenyl)-3-phenylprop-2-yn-1-one (see Fig. 1). All reagents and solvents were obtained from commercial sources and used without further purification. Starting materials included bis-(trimethylsilyl) ketene acetal **2**, which was prepared according to a published method [41] and alkynones (**1a–c**), which were prepared following the literature reported method [42]. All compounds were characterized by IR spectra, recorded on a Bruker Tensor 27 spectrometer in KBr pellets, and all data are expressed in wavenumbers (cm^{-1}). Melting points were obtained on a Melt-Temp II apparatus and are uncorrected. NMR spectra were measured with a Bruker Advance III, 300 MHz using $CDCl_3$ and DMSO-d_6 as solvents. Chemical shifts are in parts per million (δ), relative to TMS. The following abbreviations are used: s = singlet, d = doublet, t = triplet, dd = double doublet, and m = multiplet. The MS-EI spectra were obtained with an AccuTOF JMS-T100LC using 19.8 eV as the ionization energy and using ethylene glycol as a matrix. Suitable X-ray quality crystals of **3a** and **3c** were grown through slow evaporation of an ethyl acetate/*n*-hexane solvent mixture at room temperature. Single white crystals of compounds **3a** and **3c** were mounted on a glass fibre at room temperature. The crystals were then placed on a Bruker SMART APEX CCD diffractometer equipped with Mo Kα radiation. Decay was negligible in both cases. Systematic absences and intensity statistics were used in space group determinations. The structures were determined using direct methods [43]. Anisotropic structure refinements were achieved using full-matrix, least-squares techniques on all non-hydrogen atoms. All hydrogen atoms were placed in idealized positions, based on hybridization, with isotropic thermal parameters fixed at 1.2 times the value of the attached atom. Structure solutions and refinements were performed using SHELXTL v 6.10 [44].

2.1 General Procedure for the Synthesis of (2E, 4Z)-5, 7-diphenylhepta-2, 4-dien-6-ynoic Acids 3(a–c)

$BF_3{\cdot}Et_2O$ (0.44 mL, 4.44 mmol) was added to a solution of 1-(4-fluorophenyl)-3-phenylprop-2-yn-1-one (**1a**) (0.5 g, 2.22 mmol) in anhydrous diethyl ether (11.14 mL, 0.2 M) at 0 °C under a nitrogen atmosphere and stirred for 30 min. Then, we slowly added bis-(trimethylsilyl) ketene acetal **2** (0.59 mL, 2.22 mmol) at 0 °C. The reaction was stirred for 4 h at 0 °C. The reaction mixture was washed with water (11.14 mL) and extracted with dichloromethane (3 × 15 mL). The organic layer was dried over anhydrous Na_2SO_4, and the solvent was evaporated in vacuum. The crude product was purified by column chromatography on silica gel using a mixture of hexane and ethyl acetate as the eluent.

2.2 (2E,4Z)-5-(4-fluorophenyl)-7-phenyl-hepta-2,4-dien-6-ynoic Acid (3a)

A yellow solid was obtained. Chromatography column (hexane/ethyl acetate), mp 178–180 °C. IR (KBr, cm^{-1}) ν_{max}: 2988 (COO–H), 2195 (C ≡ C), 1679 (C = O) and 1594 (C = C). ^{1}H NMR (300 MHz, Acetone-d_6): δ (ppm) = 10.83 (s, COO*H*), 8.01 (dd, J = 15.3 Hz, J = 3.9 Hz, 1H, C*H*), 7.88 (ddd, J = 7.2 Hz, J = 3.9 Hz J = 2.1 Hz, 2H, C*H*), 7.61–7.56 (m, 7.32, 2H, CH), 7.43–7.38 (m, 3H, CH), 7.32 (dd, J = 11.1 Hz, J = 0.9 Hz, 1H, C*H*), 7.17 (dt, J = 8.7 Hz, J = 2.1 Hz, 2H, C*H*), 6.22 (dd, J = 15.3 Hz, J = 0.9 Hz, C*H*). ^{13}C NMR (75 MHz, $CDCl_3$): δ (ppm) = 166.88(C = O), 163.31 (J_{C-F}=246 Hz, C–F), 141.67 (CH), 133.02 (C), 131.60 (CH), 131.43 (CH), 129.37 (CH), 128.84 (C), 128.79 (CH), 128.67 (CH), 124.30 (CH), 122.31 (C), 115.6 ($J_{C\text{-}F}$ = 21.9 Hz, CH-F), 99.39 (C), 85.41 (C). MS (DART$^+$) m/z (%): 310 (10) [M^++18], 293 (100) [M^++1], 275 (28) [M^+−OH], 247 (8) [M^+−COOH]. MSHR calculated for $C_{19}H_{15}FO_2$: 293.1056, found 293.1050.

2.3 (2E,4Z)-5-(4-chlorophenyl)-7-phenyl-hepta-2,4-dien-6-ynoic Acid (3b)

A yellow solid was obtained. Chromatography column (hexane/ethyl acetate), mp 192–194 °C. IR (KBr, cm^{-1}) ν_{max}: 2968 (COO–H), 2191 (C ≡ C), 1679 (C = O) and 1606 (C = C). ^{1}H NMR (300 MHz, DMSO-d_6): δ (ppm) = 12.52 (s, COO*H*), 7.85 (dd, J = 6.9 Hz, J = 2.4 Hz, 2H, C*H*), 7.78 (dd, J = 15 Hz, J = 3.6 Hz, 1H, C*H*), 7.63–7.59 (m, 2H, CH), 7.53–7.45 (m, 6H, CH), 6.28 (dd, J = 15 Hz, C*H*), 7.17 (dt, J = 8.7 Hz, J = 2.1 Hz, 2H, C*H*), 6.22 (dd, J = 15.3 Hz, J = 0.9 Hz, C*H*). ^{13}C NMR (75 MHz, DMSO-d_6): δ (ppm) = 167.80 (C = O), 141.10 (CH), 135.25 (C), 134.47 (CH), 132.79 (CH), 131.97 (CH), 131.94 (C), 130.08 (CH), 129.42 (CH), 129.34 (CH), 128.59 (CH), 127.94 (C), 126.44 (CH), 121.95 (CH), 100.06 (C), 85.63 (C). MS (DART$^+$) m/z (%): 326 (8) [M^++18], 309 (100) [M^++1], 291 (36) [M^+−OH], 265 (24) [M^+−COOH]. MSHR calculated for $C_{19}H_{14}ClO_2$: 309.0707, found 309.0697.

2.4 (2E,4Z)-5-(4-bromophenyl)-7-phenyl-hepta-2,4-dien-6-ynoic Acid (3c)

A yellow solid was obtained. Chromatography column (hexane/ethyl acetate), mp 208–210 °C. IR (KBr, cm^{-1}) ν_{max}: 2925 (COO–H), 2201 (C ≡ C), 1679 (C = O) and 1608 (C = C). ^{1}H NMR (300 MHz, Acetone-d_6): δ (ppm) = 10.83 (s, COO*H*), 8.05 (dd, J = 15.3 Hz, J = 11.4 Hz, 1H, C*H*), 7.87 (ddd, J = 6.6 Hz, J = 2.7 Hz J = 1.8 Hz, 2H, C*H*), 7.69–7.64 (m, 7.32, 4H, CH), 7.52–7.45 (m, 4H, CH), 6.32 (dd, J = 15.3 Hz, J = 0.9 Hz, 1H, C*H*). ^{13}C NMR (75 MHz, Acetone-d_6): δ (ppm) = 166.74 (C = O), 141.45 (CH), 135.83 (C), 132.01 (CH), 131.84 (CH), 131.61 (CH), 129.42 (C), 128.80 (CH), 128.72 (CH), 128.43 (CH), 124.83 (CH), 122.92 (C), 122.25 (CH), 100.05 (C), 85.09 (C). MS (DART$^+$) m/z (%): 371 (5) [M^++18], 353 (40) [M^++1], 274 (50) [M^+−Br], 230 (100) [M^+−COOHBr]. MSHR calculated for $C_{19}H_{14}BrO_2$: 354.0255, found 354.0263.

2.5 Doping of (2E, 4Z)-5, 7-diphenylhepta-2, 4-dien-6-ynoic Acids

Indium(III) phthalocyanine chloride was used in this study to obtain molecular semiconductors. They were purchased from a commercial source and required no further purification. A series of three semiconductors were doped by a simple reaction in absolute methanol between **3a**, **3b**, **3c** and In(III)PcCl in a conventionally heated reactor (Monowave 50) with a pressure sensor. The reactor was operated with a borosilicate glass vial and manually closed by a cover with an integrated pressure (0–20 bar) and temperature sensor. 663 mg (1 mmol) of In(III)PcCl was added to 292 mg (1 mmol) of **3a** or 308 mg (1 mmol) of **3b** or 353 mg (1 mmol) of **3c**, respectively, and dissolved in methanol. These were kept in the reactor for 30 min and cooled by lowering the pressure and temperature of the system. The doped semiconductor was filtered, washed with methanol/water (1:1) and dried in vacuum. Structural characterization of these semiconductors was performed by energy-dispersive X-ray (EDS), infrared (IR) and ultraviolet-visible (UV-Vis) spectroscopies. A ZEISS EVO LS 10 scanning electron microscope was coupled to a Bruker microanalysis system and operated at a voltage of 20 kV and a focal distance of 25 mm. IR analysis was carried out using a Nicolet iS5-FT spectrophotometer and a Unicam spectrophotometer model UV300 in the wavelength range of 200–1100 nm was employed for UV-vis spectroscopy. The electrical behaviour of doped semiconductors was evaluated using the four-tips collinear

method with equal spacing and inline over simple structures. The structures was fabricated on glass substrates coated with a tin-doped In_2O_3 (ITO) film. Subsecuently buffer layer of poly(3,4-ethylenedioxythiophene)poly(styrenesulfonate) (PEDOT:PSS) were deposited by spin-coating aqueous polymer solutions, with added organic semiconductors. Film deposition was carried out in a Smart Coater 200 in the following two-step process: 300 rpm for 7 s, followed by drying at 110 °C for 30 min. ITO/PEDOT:PSS act as anode, the doped semiconductor acts as the active layer and finally, a top Ag contact was deposited as cathode. The *I(V)* behaviour were obtained using a sensing station with lighting controller circuit from Next Robotix and an auto-ranging Keithley 4200-SCS-PK1 pico-ammeter were employed.

3 Results and Discussion

3.1 Synthesis and Characterization of Dienynoic Acids as Conjugated Semiconductors

We started the study with the reaction of 1-(4-fluorophenyl)-3-phenylprop-2-yn-1-one (see Fig. 1). One mmol **1a** in dry dichloromethane at 0 ºC was added to 1.1 mmol of BF_3Et_2O. The formation of a brown solution was observed after 30 min, and subsequently was added an 1.0 mmol of ketene acetal **2** reacted for 4 h at 0 ºC. Then, the product of the reaction was washed with distilled water to remove boron waste and it was subjected to an extraction process with 3×15 mL of dichloromethane. To ensure high purity, needed for use of this compound as a semiconductor, purification of the organic phase was carried out by column chromatography with a hexane-ethyl acetate elution system. The corresponding (2*E*,4*Z*)-5-(4-fluorophenyl)-7-phenylhepta-2,4-dien-6-ynoic acid **3a** was obtained as a yellow solid in 27% yield. According to their physical data, the observed product results from the nucleophilic addition of the ketene acetal **2** to carbonyl of the ynone **1a**. In the ^{1}H NMR spectrum of **3a**, can be identified by the signal appearing at 8.01 ppm, which corresponds to the methine H13, which appears at a high frequency due to the electronic desprotection by being between double bonds, the multiplicity presented as a signal double of doubles is due to their interaction with the methines H12 and H14. Likewise, the signal corresponding to H12 can be observed at 7.41 ppm, as a double signal with a coupling constant of $J = 11.1$ Hz. The proton H14 appears also with as double signal to 6.24 ppm, with coupling constant of $J = 15.3$ Hz. The value of both constants gives information about the configuration of the system, because by being the methines in trans position, the stereochemistry of the molecule most be (*E, Z*), confirming that the thermodynamic product is obtained. Another characteristic signal of the system is the wide signal at 10.80 ppm, which corresponds to the proton of the carboxylic acid. The other signals correspond to the two aromatic systems, both the disubstituted and the monosubstituted. The ^{13}C NMR spectra confirmed the incorporation of a carboxylic acid by the signal appearing at 166.88 ppm and the signal at 99.93 ppm and 85.41 ppm correspond to the alkyne. These signals give certainty that the triple bond was not compromised in the process of nucleophilic addition of the ketene acetal to the ynona **1a**, which is of great benefit since there is a conjugated system and the presence of a halogen allows for a *push-pull* system (Fig. 2), where the carbonyl can pull electronic density, and the triple bond can donated electronic density for compensate in part the electronic delocation. Since the halogens have the particularity to be an electron donating group by resonance and electron withdrawing group by inductive effect, they can be generated a molecule with semiconductor properties behaviour.

To carry out a more precise elucidation of the structure of **3a**, an IR spectroscopy study took place. In the spectrum, the presence of functional groups in the molecule in question could be observed. The vibration correspondent to carboxylic acid COO–H is observed in 2968 cm^{-1}. The triple bond was evident with a low intensity band at 2191 cm^{-1}, typical of an internal alkyne. The bands correspondent to stretch vibrations for a double bond C = O of carboxylic acid appears at 1679 cm^{-1} and the vibrations of the doubles bonds C = C are observed 1606 cm^{-1}. Due to the intensity of this band, it is possible that the signal of both double bonds overlapped, it is possible to mention that corresponds to a conjugated dyeno, since it's in the characteristic zone for this type of systems. Additionally, the mass spectrometry

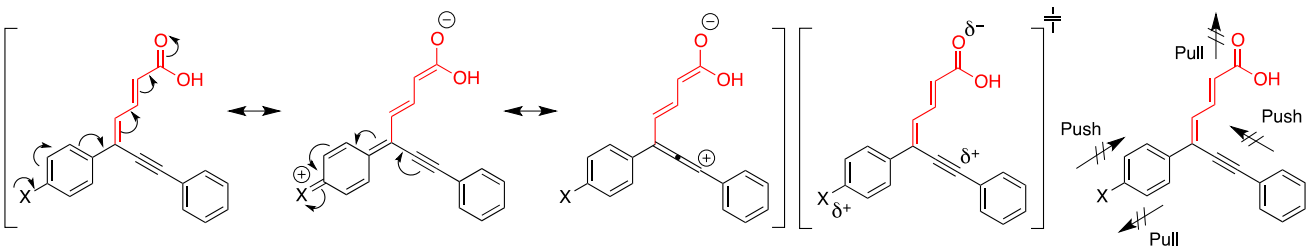

Fig. 2 Push-pull systems of (2E, 4Z) dienynoic acids

analysis by means of the $DART^+$ technique was carried out, observing the base peak at 293 m/z, corresponding to [M + 1] when using an indirect ionization method. Access is given to the molecular ion plus a hydrogen and the molecular ion plus ammonium [M + 18], which is obtained in the peak at 310 m/z. Peaks of higher m/z ratios are not observed. This suggests that compound **3a** presents a high degree of purity. Finally, the peaks observed by HRMS ($DART^+$) at 293.1050 *m/z* confirmed the expected masses, in accordance with their calculated mass of 293.1056 and the molecular formula of $C_{19}H_{14}FO_2$. Suitable X-ray quality crystals of **3a** were grown through slow evaporation of an ethyl acetate/*n*-hexane solvent mixture at room temperature. The structure of **3a** was verified by X-ray analysis (Fig. 3a; Table 1). **3a** showed a special group P 21/n in a monocyclic crystalline system, and the structural disposition showed the formation

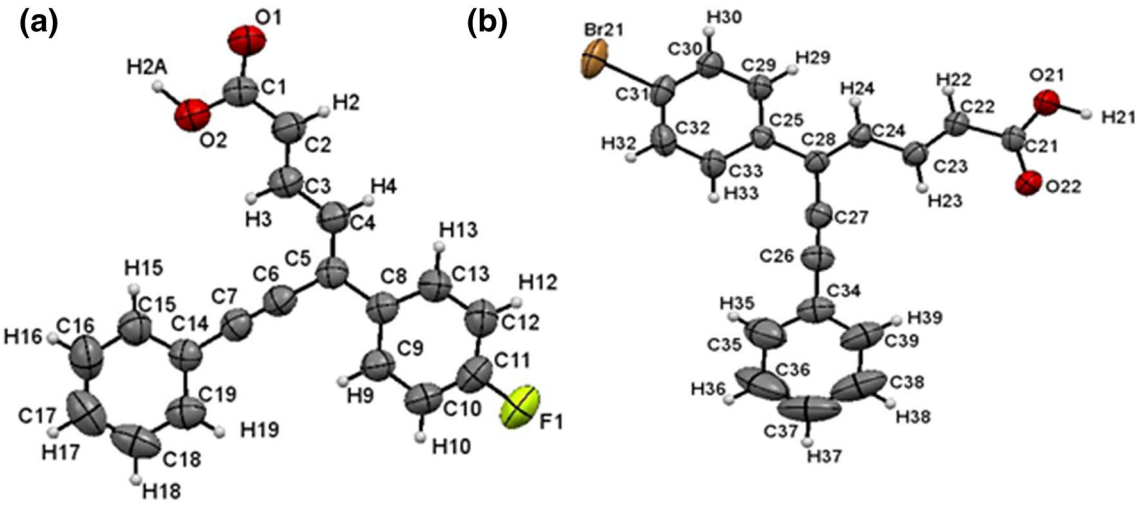

Fig. 3 ORTEP of structure of (**a**) **3a** and (**b**) **3c**. Thermal ellipsoids at 50% probability level

Table 1 Crystal data and structure refinement for **3a** and **3c**

Compound	3a	3c
Empirical Formula	$C_{19}H_{13}FO_2$	$C_{19}H_{13}BrO_2$
Formula Weight (g mol^{-1})	292.29	353.20
Cristal size (nm)	0.374 × 0.230 × 0.217	0.36 × 0.18 × 0.18
Color	Yellow	Yellow
Cristal system	Monoclinic	Orthorhombic
Space group	P 21/n	Pna2
a (Å)	5.9471(3)	13.6906(16)
b (Å)	21.8990(9)	31.234(4)
c (Å)	11.8841(5)	7.6144(8)
α (°)	90	90
β (°)	98.818	90
γ (°)	11.8841	90
V ($Å^3$)	1529.44(12)	3256.0(6)
D_{calc} (g cm^3)	1.269	1.441
Z	4	8
Number of collected reflections	27333	35969
Number of independent reflections	4287, R_{int} = 0.0540	9482, R_{int} = 0.073
Maximum and minimum transmission	0.959 and 0.9705406	0.63 and −0.33
Data/restraints/parameters	8/30/16	8/30/16
Final R índices [$l > 2\sigma > l$)]	R = 0.0540 $wR2$ = 0.1241	R = 0.053 $wR2$ = 0.109
R indices (all data)	R = 0.0996 $wR2$ = 0.1499	R = 0.0996 $wR2$ = 0.1499
Absorption correction method	Multi-scan	Multi-scan

of dienynoic acid in conformation (*E, Z*). Geometric parameters of the bond distance for C–O in carbonyl and hydroxyl showed good differentiation, with a distance of 1.242(19) Å for the carbonyl and 1.289(2) Å for the hydroxyl. On the other hand, the bond distances of alkenes show a slightly difference respect to their elongation, being the nearest to the carboxyl, that of shorter length 1.327(2) Å, respect to the other double bond of 1.352(2) Å. However, both bond distances are in the range of acceptable parameters for a double bond. With respect to the triple bond, it has a length of C≡C of 1.196(2) Å, very coherent distance for this type of bond. Also, the intermolecular interactions that these molecules present can be analysed, making the hydrogen bridge type interaction evident between the hydroxyl of a carboxylic acid and the carbonyl of the same molecule O_1–H_{2A}–O_2, with distance of 1.09(2) Å. Finally, an intermolecular interaction can be observed, now between the oxygen of a carboxylic acid with the proton of one of the aromatic rings of another molecule (C_{12}–H_{12}–O_1), with an elongation of 0.93 Å. These types of interactions are common in molecules of carboxylic acids due to their trend to form dimers in their crystalline structure.

Subsequently, we explored this reaction of due different aryl ynones **1** bearing Cl and Br substituents reacted with **2**, which led to the formation of compounds **3b** and **3c** (see Fig. 1) in yields of 63% and 75%, respectively. Both synthetized dienynoic acids showed similar properties, even when the halogen atom was changed. All are yellow crystalline solids, with low solubility in polar solvents such as ethyl acetate, ethanol, and methanol. This could be because the carboxylic acids tend to form dimeric structures, which provides stability to their crystalline lattice. In the ORTEP projection of compound **3c** shown in Fig. 3b; Table 1, the formation of an intermolecular dimer can be seen. However, the use of polar solvents, not protic solvents, such as dimethylformamide or dimethylsulfoxide, allows for proper solubility, perhaps because this type of intermolecular interaction is diminished by providing excellent solvation. On the other hand, the melt points were measured; all acids have high thermal stability with melt points around 200 °C (188, 182, and 200 °C for **3a**, **3b**, and **3c**, respectively). Since the physical properties of compounds **3b** and **3c** are similar, only the crystalline structure of **3c** will be described and analysed by X-ray diffraction (XRD) (Fig. 3b; Table 1). The proper monocrystal was obtained from an *n*-hexane-ethyl acetate solution. The structural arrangement showed the formation of dienynoic acid with (*E, Z*) conformation of the double bonds. Crystallized in a special group ($Pna2_1$) in an orthorhombic crystalline system, the geometric parameters of the bond distances for C–O of the carbonyl and the hydroxyl show good differentiation to a 1.257(6) Å distance for the carbonyl and 1.286(7) Å distance for hydroxyl. On the other hand, the bond distances show slight differences with respect to their elongation, being the nearest to the carboxyl, that of shorter length 1.324(7) Å, respect to the other double bond with a distance of 1.346(7) Å. However, both bond distances are in the range for the acceptable parameters for a double bond. With respect to the triple bond, it has an elongation of 1.188(7) Å, which is a very coherent distance for this type of bond. On the other hand, the hydrogen bond geometry shows the intermolecular interaction between the carbonyl and hydroxyl (O_1–H_1–O_{22}) of two different molecules of acid **3c**, with a distance of 0.99(6) Å and O_{21}–H_{21}–O_2 with a distance of 1.01(7) Å. These are characteristic of the marked tendency of the acids to form dimers. Details about crystallographic information are provided in the supporting information.

It is important to note that all diene products were obtained in geometrically pure (*E, Z)*-configurations, highlighting the mildness of the reaction conditions and the simplicity of the procedure. The proposed pathway of this Mukaiyama-type aldol reaction begins with the formation of intermediate **A** by the nucleophilic addition of ketene acetal **2** to the ynone **1**; the dehydration of intermediate **A** gives the corresponding dienyne **B**. Finally, intermediate **B** can undergo hydrolysis, leading to the formation of suitable dienynoic acid **3**. Although the yield of the reaction is moderated, the molecular materials obtained present high purity, proven by the NMR, mass spectrometry, and XRD results. Impurities in organic semiconductors for applications in electronic devices are undesirable because they may act as traps for charges, resulting in a decrease in average mobility. Due to the information above, two main approaches are currently used to obtain high purity organic semiconductors: simplification/optimization of synthetic routes or repeated purification of the final products. The synthesis proposed in the present study to obtain **3a**, **3b**, and **3c** is not only simplified, but the purification by chromatography performed in the three compounds generates the expected purity.

3.2 Doping of Semiconductors

The molecular doping carried out consisted of mixing each acid with In(III)PcCl to shorten the distance between the two species, electron-donor and electron-acceptor, and to ease the electronic transfer between both. During doping, the dienynoic acid was unpurified with In(III)PcCl in a way that could favour electronic transfer by the mixed bulk heterojunction, (BHJ), giving place to a random distribution between the acid and the phthalocyanine and increasing their contact surfaces. The BHJ is formed by the mixture of these compounds in absolute methanol, which generates dispersed phases and interconnects one to the other, amongst which there is a greater contact surface [45]. The supramolecular interaction is through weak bonds van der Waals. These bonds form segregated blocks with intermolecular

overlap in which the spacing between the molecules generates bands through which conduction channels are formed. The doped materials, named **3a′:InPcClF**, **3b′:InPcClCl**, and **3c′:InPcClBr**, were analysed by IR spectroscopy to monitor the chemical structure of the dienynoic acid and the In(III)PcCl. The signs referring to dienynoic acids are at 2968 cm^{-1} for the vibration of COO–H, 2191 cm^{-1} for the internal alkyne, 1679 cm^{-1} for the vibration of C = O, and 1606 cm^{-1} for the C = C bond. With respect to InPcCl, the bands responsible for C = N appear at 1481, 1334, and 1279 cm^{-1}, while the bands located around 1160, 1119, and 748 cm^{-1} result from the interaction of C–H [46, 47]. On the other hand, from IR spectroscopy it is possible to identify the different crystalline structures, α and β, in Pcs [48]. The α-form of Pc can be characterized by a band around 720 cm^{-1}, while the β-form can be characterized by one band around 778 cm^{-1} [49]. Table 2 shows the characteristic signs for each doped material, **3a′:InPcClF**, **3b′:InPcClCl**, and **3c′:InPcClBr**, and as can be seen, in all cases are present a mixture of Pc, in α-form, as well as in β-form. Based on the IR spectroscopy results, it is observed that doping with In(III)PcCl was performed properly, so efficient charge transport between both molecules joined by BHJ is expected. On the other hand, IR spectroscopy did not detect the presence of external impurities that could affect charge transport.

The organic semiconductors **3a′:InPcClF**, **3b′:InPcClCl**, and **3c′:InPcClBr**, were analysed by SEM and EDS to verify the presence of the chemical elements of the doped semiconductors. In all cases, the presence of indium, nitrogen, and chlorine from Pc and the oxygen and the halogens F, Cl, or Br from dienynoic acid was found. The results of SEM and EDS for **3b′:InPcClCl** are shown in Fig. 4, similar results were obtained for the rest of the semicondutors. The dienynoic acids and In(III)PcCl integrate the organic semiconductors and they are responsibles for the generation of the charge carriers. The BHJ favour and increase the contact surface acid/In(III)PcCl that contributes to the transition of electron-hole pairs. UV-vis spectroscopy was carried out in order to analyse the electronic transitions that could take place within the molecular semiconductors. Figure 5 shows the absorption spectra for each dienynoic acid pure and doped. The absorbance value is practically the same for pure acids; however, the most significant spectral properties are caused by In(III)PcCl and its aromatic cyclic conjugated 18-π-electron system. The spectrum shows: the *B*-band in the near UV region and the *Q*-band on the red side of the spectrum. The doped semiconductors have the *B*-band around 350 nm [47]. The electronic $n-\pi^*$ transition corresponds to a *B*-band, which gives the fundamental absorption edge. The *B*-band is due to $a_{2u}(\pi) \rightarrow e_g(\pi^*)$ together with $b_{2u}(\pi) \rightarrow e_g(\pi^*)$ transitions [50]. Additionally in the UV-vis spectra of Fig. 5a peak is observed around 650 nm, this corresponds to the *Q*-band of the In(III)PcCl, assigned to the first π-π^* transition on the Pc macrocycle [47, 51]. The

Table 2 IR spectroscopy characteristic bands for doped materials.

Sample	COO-H ν (cm^{-1})	C≡C ν (cm^{-1})	C = O ν (cm^{-1})	C = C ν (cm^{-1})	C = N ν (cm^{-1})	C-H ν (cm^{-1})	α-form ν (cm^{-1})	β-form ν (cm^{-1})
3a′:InPcClF pellet	2969	2191	1678	1610	1481, 1334, 1284	1163, 1118, 748	720	780
3b′:InPcClCl pellet	2970	2203	1681	1608	1484, 1338, 1281	1161, 1114, 748	720	780
3c′:InPcClBr pellet	2973	2206	1694	1609	1480, 1335, 1284	1162, 1117, 748	720	780

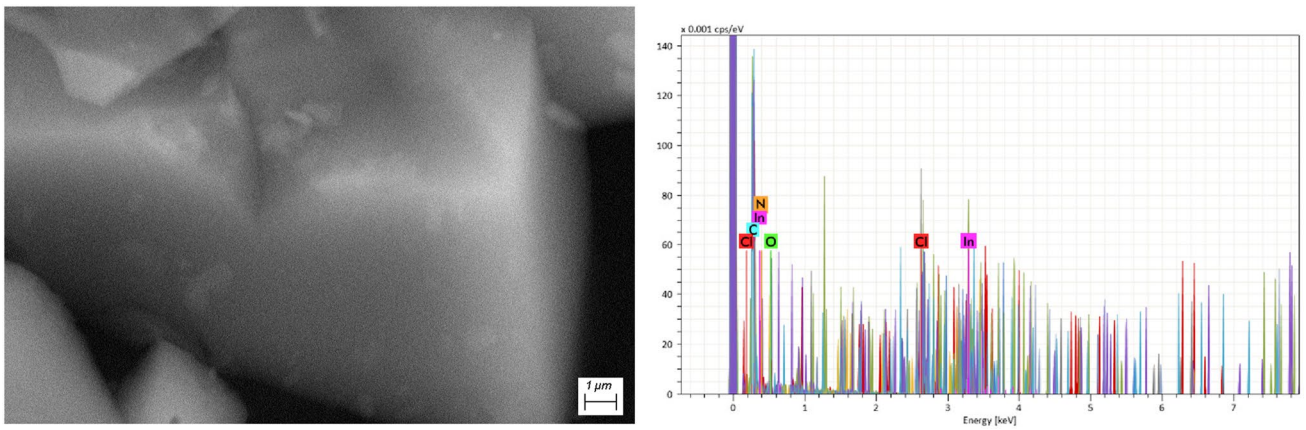

Fig. 4 SEM image at 15000x and EDS spectrum for **3b′:InPcClCl** semiconductor

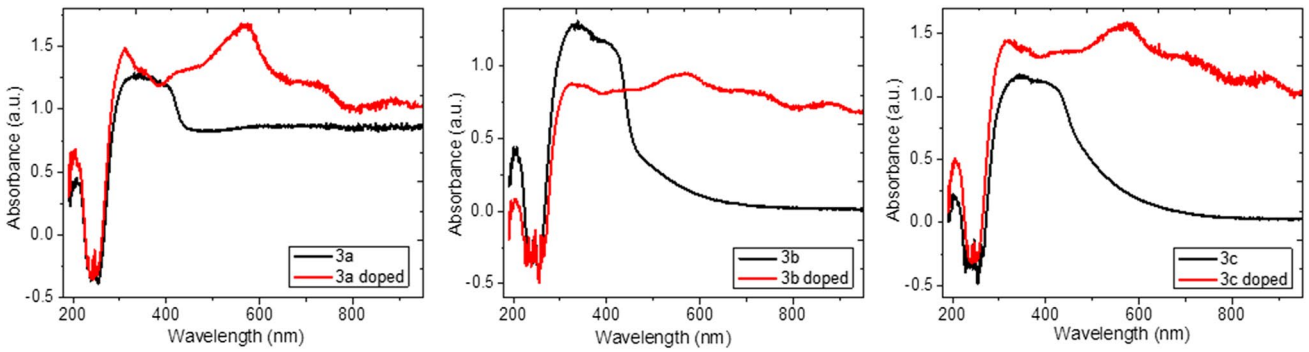

Fig. 5 UV-vis spectroscopy of dienynoic acids pure and **3a′:InPcClF**, **3b′:InPcClCl** and **3c′:InPcClBr** doped

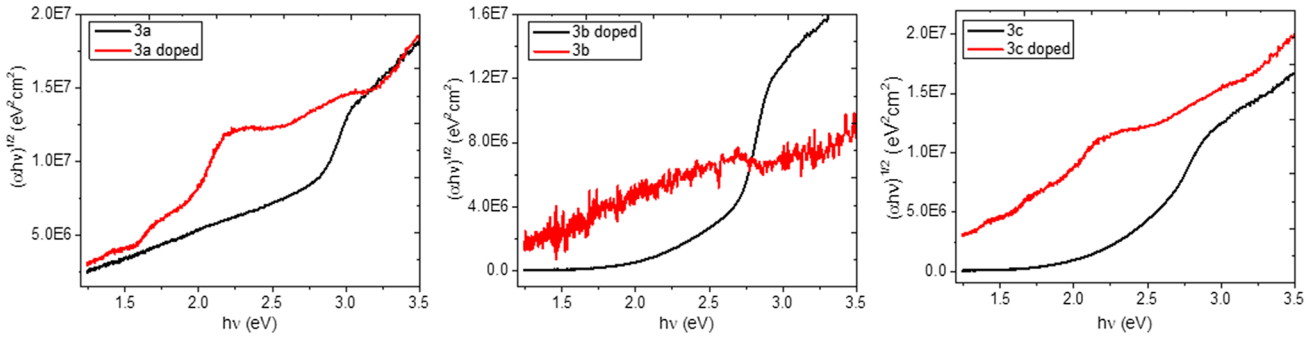

Fig. 6 Absorption curves showing the transitions that correspond to optical bandgaps of dienynoic acids pure and **3a′:InPcClF**, **3b′:InPcClCl** and **3c′:InPcClBr** doped

Q-band is localized on the Pc ring and is sensitive to the environment of the molecule [52]. It is possible to observe in the spectra that around 500 nm, absorption bands are recorded by electron donation process between the ligand and the metal center.

In addition to obtaining the Q and B bands, UV-vis spectroscopy was used to obtain the optical bandgap (E_g). The bandgap characterizes the electronic behaviour of the material, in organic semiconductors, the difference in energy between the HOMO (highest occupied molecular orbital) and the LUMO (lowest unoccupied molecular orbital), or E_g, is located around 1.5–4.0 eV, which makes charge transport possible and thus their use in optoelectronic devices. The E_g of each dienynoic acid doped was obtained using Tauc's semi-empiric method, used for amorphous semiconductor [53]. The E_g was obtained from (i) the evaluation of absorbance and transmittance from UV-vis spectroscopy, (ii) the calculation of absorption coefficient (α) and (iii) the calculation of photon energy ($h\nu$). E_g should be determined by extrapolating the linear trend observed in the spectral dependence of $(\alpha h\nu)^{1/2} = f(h\nu)$ over the axis of photon energy [53] (see Fig. 6). Table 3 shows the E_g values obtained of each dienynoic acid doped. It should be mentioned that to determine the effect of In(III)PcCl, the E_g for compounds **3a**, **3b**, and **3c** without doping was obtained. It is important to observe how the In(III)PcCl and the BHJ significantly diminishes the value of E_g from **3a´:InPcClF** and **3c´:InPcClCl**, from values between 2.35–2.6 eV obtained for pure compounds to values near 1.4–1.7 eV for the same compounds but now with Pc doping. In the case of **3b** the presence of In(III)PcCl is evident, since apparently the behavior of acid **3b** changes to semiconductor with 2.60 eV bandgap. E_g for molecular semiconductors has typical values between 1.5 and 4.0 eV, so the results obtained are within the expected range. However the evaluation of the electrical behavior of the organic semiconductors provides complementary information to establish the usability or non-usability of this molecular semiconductors in optoelectronic

Table 3 Optical bandgap (E_g) for pure and doped dienynoic acids

Sample	E_g (eV)
3a	2.60
3b	–
3c	2.35
3a′:InPcClF	1.70
3b′:InPcClCl	2.60
3c′:InPcClBr	1.41

applications. Until now it has been considered that the molecular semiconductor **3a′:InPcClF**, **3b′:InPcClCl**, and **3c′:InPcClBr** are in equilibrium; however, besides evaluating their electric behaviour in dark conditions, they were illuminated with electromagnetic radiation in order to carry out the excitation of charge carriers and for each absorbed photon, generating an electron-hole pair. Additionally, thanks to the BHJ inside the semiconductor doped, there is a transfer of carriers from one semiconductor to another (from dienynoic acid to In(III)PcCl), which is verified from the E_g values obtained (reported in Table 3).

The current-voltage *I(V)* relationship of each molecular semiconductor was evaluated using ITO/PEDOT:PSS as the anode [54, 55], **3a′:InPcClF**, **3b′:InPcClCl** and **3c′:InPcClBr** as the active layer and Ag as the cathode. From *I(V)* evaluations in lighting conditions as well as in dark conditions, the current density (*J*) transported in each structure was determined. The forward and reverse biased *J(V)*, characteristic of the structures at room temperature, are exhibited in Fig. 7. Figure 7a shows the *J(V)* graphic for the ITO/PEDOT:PSS/Ag structure in order to establish a comparative study between **3-InPcCl** semiconductors and the PEDOT:PSS. It is evident that the presence of the doped semiconductor **3-InPcCl** modifies the transport properties. The *J*(*V*) graphs of the structures with active layers of **3a′:InPcClF** and **3b′:InPcClCl** (Fig. 7b and c, respectively) in the dark and under illumination show the typical form of organic semiconductors in diode-type devices. It is worth observing how the curves obtained under lighting conditions show higher current transported at voltages greater than 0.5 V, which indicates slight photovoltaic behaviour. The shape of the curve is usually related to imbalances in charge mobilities [56] the presence of interfacial poles [57] energy barriers in the interphase with the active layer and the electrode [58–60], as well as limitations in the charge transport [61]. In the present study, it is considered that the shape of the *J(V)* curve added to the slope change in 0.8 and 0.5 V for the structures with the layer **3a′:InPcClF** and **3b′:InPcClCl**, respectively, is an indication of the change of charge transport regime from ohmic at low voltages, to the controlled by a current type SCLC (space charge limited current). This change in the charge transport regime is associated with the charge accumulation inside the structure. Although, according to the graphics of Fig. 7, the rectification mechanism is not present in the structures; asymmetry is observed in the curves, which indicates the importance of the electrodes

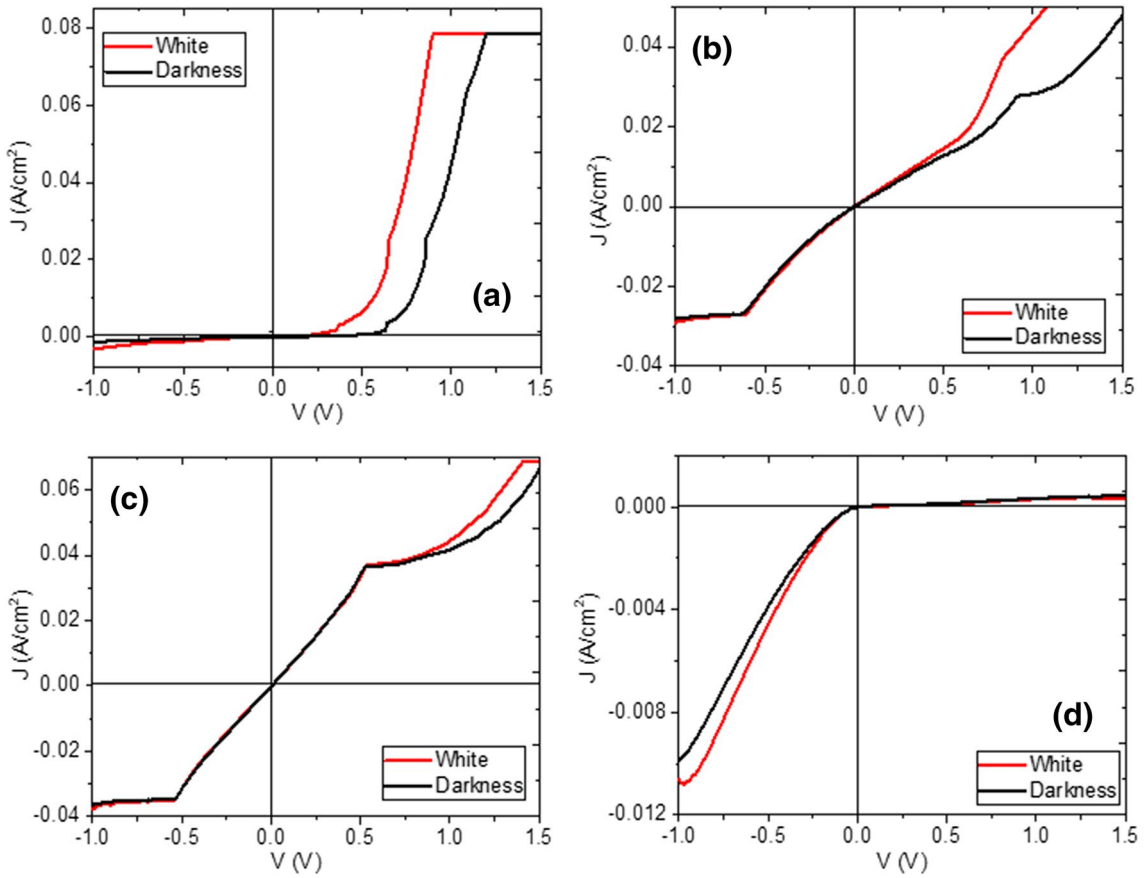

Fig. 7 *J* versus *V* plot of the (**a**) PEDOT:PSS, (**b**) **3a′:InPcClF**, (**c**) **3b′:InPcClCl** and (**d**) **3c′:InPcClBr**

used as the cathode and anode because the electronic transport changes slightly. Since the change in semiconductor **3a′:InPcClF** and **3b′:InPcClCl** is not significant, it could be assumed that their behaviour is ambipolar. With respect to the structure manufactured from the dienynoic acid with bromine **3c′:InPcClBr** (see Fig. 7d), insulating behaviour is observed by exchanging the polarity of the structure. Yet, in the third quadrant of the graphic, the behaviour is ohmic. Finally, it is possible to observe that although the differences are small, the structure **3b′:InPcClCl** is the one that transports highest current density.

4 Conclusions

The new (2E, 4Z)-5, 7-diphenylhepta-2, 4-dien-6-ynoic acids were chemically and structurally synthetized and characterized. These compounds were doped with In(III) PcCl in order to generate molecular semiconductors. The optic bandgap of these semiconductors was evaluated by UV-Vis spectroscopy, and the values found ranged from 1.4 to 2.6 eV. When comparing the optical bandgap of the doped semiconductors to the bandgap of pure acids, a decrease in the bandgap values is observed. The heterojunction with In(III)PcCl diminishes the value of E_g. With the doped semiconductor obtained were manufactured structures of disperse heterojunction which later were enhanced in their electric behavior. A behaviour ohmic at low voltages and Space Charge Limited Current (SCLC) at higher voltages was observe from the study *J(V)* carried out. However in all cases, the behaviour of the structures is similar to an organic diode and the (2E, 4Z)-5, 7-diphenylhepta-2, 4-dien-6-ynoic acids can used in optoelectronic devices.

Acknowledgements The authors wish to thank the technical assistance of Rocío Patiño, Saulo C. Rosales, Santiago Inestrillas Hernández, Jackeline Guadalupe Herrera Osuna, Karen Fernanda González Reyes, and IN4. The authors gratefully acknowledge the financial support of CONACYT-México, under the Project Number 252020, and the DGAPA-PAPIIT Project Number IN202917. We would also like to thanks the CONACYT for the Ph.D. grant extended to R. B. I. and M.E.S.V. acknowledges the financial support from Anahuac México University, Project Number NNAIASEVM16070616.

References

1. A. Tsumura, K. Koezuka, T. Ando, Macromolecular electronic device: field-effect transistor with a polythiophene thin film. Appl. Phys. Lett. **49**, 1210–1212 (1986)
2. S. Ren, N. Zhao, S.C. Crawford, M. Tambe, V. Bulovic, S. Gradecak, Heterojunction photovoltaics using GaAs nanowires and conjugated polymers. Nano Lett. **11**, 408–413 (2011)
3. Y. Zhou, M. Eck, M. Kruger, Bulk-heterojunction hybrid solar cells based on colloidal nanocrystals and conjugated polymers. Energy Environ. Sci. **3**, 1851–1864 (2010)
4. S.K. Shahenoor, G.S. Sundari, K.V. Kumar, M.C. Rao, Structural and dielectrical properties of PVP based composites polymer electrolyte thin films. J. Inorg. Organomet. Polym. **27**, 455–466 (2017)
5. S. Mansurova, D. Nolte, I. Seres, S. Stepanov, R. Ramos, J. Appl. Phys. **92**, 1825–1832 (2002)
6. M.C. Gather, S. Mansurova, K. Meerholz, Determining the photoelectric parameters of an organic photoconductor by the photoelectromotive-force technique. Phys. Rev. B **75**, 165203 (2007)
7. K. Sasikumar, R. Bharathikannan, J. Chandrasekaran, M. Raja, Effect of organic additives on the characteristics of Al/organic additive: ZrO2/p-Si metal-insulator-semiconductor (MIS) type schottky barrier diodes. J. Inorg. Organomet. Polym. (2019). https://doi.org/10.1007/s10904-019-01216-x
8. M. Furber, J.M. Herbert, R.J. Taylor, Stereoselective synthesis of 2Z, 4E-dienats by addition of organometallic reagents to pyrylium perchlorate. J. Chem. Soc. **1**(4), 683–690 (1989)
9. K.C. Nicolaou, R.E. Zipkin, R.E. Dolle, B.D. Harris, A general and stereocontrolled total synthesis of leukotriene B4 and analogues. J. Am. Chem. Soc. **106**, 3548–3552 (1984)
10. G. Wald, The molecular basis of visual excitation. Nature **219**, 800–807 (1968)
11. C.E. Orfanos, R. Ehlert, H. Gollnick, The retinoids. Drugs **34**, 459–503 (1987)
12. L. Eyrolles, E. Kawachi, H. Kagechika, Y. Hashimoto, K. Shudo, Synthesis and biological activity of carboxyphenylquinolines and related compounds as new potent retinoids retinobenzoic acids. Chem. Pharm. Bull. **42**, 2575–2580 (1994)
13. A. Wada, S. Hiraishi, N. Takamura, T. Date, K. Aoe, M. Ito, A novel method for a stereoselective synthesis of trisubstituted olefin using tricarbonyliron complex: a highly stereoselective synthesis of (all-E)- and (9Z)-retinoic acids. J. Org. Chem. **62**, 4343–4348 (1997)
14. A. Matsumoto, K. Sada, M.M. Tashiro, T. Tsubouchi, T. Tanaka, T. Odani, S. Nagahama, T. Tanaka, T.I. Katsunari, S. Saragai, S. Nakamoto, Reaction principles and crystal structure design for the topochemical polymerization of 1,3-dienes. Angew. Chem. Int. Ed. **41**, 2502–2505 (2002)
15. C. Souris, M. Luparia, F. Frédéric, D. Ausidisio, C. Farès, R. Goddard, N. Maulide, An atom-economical and stereoselective domino synthesis of functionalised dienes. Chem. Eur. J. **19**, 6566–6570 (2013)
16. C. Souris, M. Luparia, F. Frédéric, D. Ausidisio, C. Farès, N. Maulide, Direct domino synthesis of azido-dienoic acids: potential linker units. Synlett **24**(10), 1286–1290 (2013)
17. M. Julia, B. Badet, D. Uguen, A. Callipolitis, Bull Soc Chim Fr, (1976) 513–518
18. P. Chabardes, J.P. Decor, J. Varagnat, Elimination de groupements arysulfonyles en milieu heterogene. Tetrahedron **33**, 2799–2805 (1977)
19. K. Uneyama, S. Torii, Alicyclic terpenoids from cyclocitryl phenyl sulfides IV synthesis of methyl esters of vitamin A1 and A2 acids and their geometric isomers. Chem. Lett. **6**, 39–40 (1977)
20. E. Vedejs, J.P. Bershas, A new route to stabilized ylides: a one-pot polyene synthesis. Tetrahedron Lett. **16**, 1359–1362 (1975)
21. M. Alami, B. Crousse, G. Linstrumelle, L. Mambu, Larchevêque M (1993) Total stereocontrolled synthesis of lipoxin B4. Synlett **03**, 217–218 (1993)
22. J.K. Stille, The palladium-catalyzed cross-coupling reactions of organotin reagents with organic electrophiles. Angew. Chem. Int. Ed. **25**, 508–524 (1986)
23. J.K. Stille, B.L. Groh, Stereospecific cross-coupling of vinyl halides with vinyl tin reagents catalyzed by palladium. J. Am. Chem. Soc. **109**, 813–817 (1987)
24. T.N. Mitchell, Palladium-catalysed reactions of organotin compounds. Synthesis **9**, 803–815 (1992)

25. V. Farina, V. Krishnamurthy, W.J. Scott, The stille reaction. Org. React. **50**, 1–61 (1997)
26. M. Abarbri, J.L. Parrain, A. Duchêne, J. Tribonnet, Stereoselective synthesis of trienoic acids: synthesis of retinoic acids and analogues. Synthesis **17**, 2951–2970 (2006)
27. J. Barluenga, G.P. García, D. De, M.A. Sáa, R.B. Fernández, A. De la Rúa, E. Ballesteros, M. Aguilar, Tomás, Chromium(0) alkynylcarbene complexes as Cβ-electrophilic carbene equivalents: regioselective access to dienynes and dienediynes. Angew. Chem. Int. Ed. **46**, 2610–2612 (2007)
28. Q. Tang, Y. Tong, W. Hu, Q. Wan, T. Bjørnholm, Assembly of nanoscale organic single-crystal cross-wire circuits. Adv. Mater. **21**, 4234–4237 (2009)
29. A. Facchetti, Y. Deng, A. Wang, Y. Koide, H. Sirringhaus, T.J. Marks, R.H. Friend, Tuning the semiconducting properties of sexithiophene by α,ω-substitution-α,ω-diperfluorohexylsexithiophene: the first n-type sexithiophene for thin-film transistors. Angew. Chem. Int. Ed. **39**, 4547–4551 (2000)
30. A. Facchetti, M.H. Yoon, C.L. Stern, H.E. Katz, T.J. Marks, Building blocks for n-type organic electronics: regiochemically modulated inversion of majority carrier sign in perfluoroarene-modified polythiophene semiconductors. Angew. Chem. Int. Ed. **42**, 3900–3903 (2003)
31. A. Facchetti, M.H. Yoon, C.L. Stern, G.R. Hutchison, M.A. Ratner, T.J. Marks, Building blocks for N-type molecular and polymeric electronics. Perfluoroalkyl- versus alkyl-functionalized oligothiophenes (nTs; n = 2–6). Systematic synthesis, spectroscopy, electrochemistry, and solid-state organization. J. Am. Chem. Soc. **126**, 13480–13501 (2004)
32. M.H. Yoon, S.A. DiBenedetto, A. Facchetti, T.J. Marks, Organic thin-film transistors based on carbonyl-functionalized quaterthiophenes: high mobility N-channel semiconductors and ambipolar transport. J. Am. Chem. Soc. **127**, 1348–1349 (2005)
33. R. Schmidt, J. Hak Oh, Y.S. Sun, M. Deppisch, A.M. Krause, K. Radacki, H. Braunschweig, M. Konemann, P. Erk, Z. Bao, F. Würthner, High-performance air-stable n-channel organic thin film transistors based on halogenated perylene bisimide semiconductors. J. Am. Chem. Soc. **131**, 6215–6228 (2009)
34. M. Gsänger, J. Hak Oh, M. Könemann, H. Wölfgang Höffken, A.M. Krause, Z. Bao, F. Würthner, A crystal-engineered hydrogen-bonded octachloroperylene diimide with a twisted core: an n-channel organic semiconductor. Angew. Chem. Int. Ed. **49**, 740–743 (2010)
35. O.L. Osifeko, T. Nyokong, Effects of symmetry and the number of positive charges on the photocatalytic activity of indium phthalocyanines when embedded in electrospun fibers. Inorg. Chim. Acta **458**, 50–57 (2017)
36. M.A. Köksoy, B. Köksoy, M. Durmus¸, M. Bulut, Preparation, characterization and photophysicochemical properties of novel tetra 7-(diethyl 2-methylmalonatoxy)-3-(p-oxyphenyl) coumarin-substituted zinc(II) and indium(III)chloride phthalocyanines. J. Organomet. Chem. **822**, 125–134 (2016)
37. A.M. Sevim, H.Y. Yenilmez, M. Aydemir, A. Koca, Z.A. Bayır, Synthesis, electrochemical and spectroelectrochemical properties ofnovel phthalocyanine complexes of manganese, titanium and indium. Electrochim. Acta **137**, 602–615 (2014)
38. I. Özçeşmeci, A. Gelir, A. Gül, Synthesis and photophysical properties of indium(III) phthalocyanine derivatives. J. Lumin. **147**, 141–146 (2014)
39. M. Hanack, D. Dini, M. Barthel, S. Vagin, Conjugated macrocycles as active materials in nonlinear optical processes: optical limiting effect with phthalocyanines and related compounds. Chem. Rec. **2**, 129–148 (2002)
40. Y. Liu, Y. Chen, L. Cai, J. Wang, Y. Lin, J.J. Doyle, J.W. Blau, Optical limiting properties of axially substituted indium phthalocyanines in the solid PMMA composite films. Mater. Chem. Phys. **107**, 189–192 (2008)
41. C. Ainsworth, Y. Kuo, Ketene alkyltrialkylsilyl acetals: synthesis, pyrolysis and NMR studies. J. Organomet. Chem. **46**, 59–71 (1972)
42. T. Zhao, B. Xu, Palladium-catalyzed tandem amination reaction for the synthesis of 4-quinolones. Org. Lett. **12**, 212–215 (2010)
43. A. Altomare, G. Cascarano, C. Giacovazzo, A. Guagliardi, M.C. Burla, G. Polidori, M. Canalli, A program for automatic solution of crystal structures by direct methods. J. Appl. Crystallogr. **27**, 435–436 (1994)
44. G.M. Sheldrick, Acta Crystallogr. Sect. A **64**, 112 (2008)
45. A.J. Heeger, 25th anniversary article: bulk heterojunction solar cells: understanding the mechanism of operation. Adv. Mater. **26**, 10–28 (2014)
46. N. Touka, H. Benelmadjat, B. Boudine, O. Halimi, M. Sebais, Copper phthalocyanine nanocrystals embedded into polymer host: preparation and structural characterization. J. Assoc. Arab. Univ. Basic Appl. Sci. **13**, 52–56 (2013)
47. M.M. El-Nahass, K.F. Abd-El-Rahman, A.A. Al-Ghamdi, M. Asiri, Optical properties of thermally evaporated tin-phthalocyanine dichloride thin films, SnPcCl2. Phys. B **344**, 398–406 (2004)
48. Hart MM (2009) Cationic exchange reactions involving dilithium phthalocyanine. Thesis for the degree of Master of Science, Wright State University, (2009)
49. L. Galfo, M.R. Cordeiro, A.R. Freitas, W.C. Moreira, E.M. Girotto, V. Zucolotto, The effects of temperature on the molecular orientation of zinc phthalocyanine films. J. Mater. Sci. **45**(3), 1366–1370 (2010). https://doi.org/10.1016/S0043-1354(02)00276-2
50. M. Novotny, J. Bulir, A. Bensalah-Ledoux, S. Guy, P. Fitl, M. Vrnata, J. Lancok, B. Moine, Optical properties of zinc phthalocyanine thin films prepared by pulsed laser deposition. Appl. Phys. A **117**, 377–381 (2014)
51. M.M. El-Nahass, A.M. Farag, K.F.A. El-Rahman, K.F.A. Darwish, Dispersion studies and electronic transitions in nickel phthalocyanine thin films. Opt. Laser Technol. **37**, 513–523 (2005)
52. M.M. El-Nahass, M. Sallam, H.A.M. Ali, Optical properties of thermally evaporated metal-free phathalocyanine (H2Pc) thin films. Int. J. Mod. Phys. B **27**, 4057–4071 (2005)
53. J. Tauc, Optical properties and electronic structure of amorphous Ge and Si. Mater. Res. Bull. **3**, 37–46 (1968)
54. J. Ouyang, C.-W. Chu, F.-C. Chen, Q. Xu, Y. Yang, High-conductivity poly(3,4-ethylenedioxythiophene): poly(styrene sulfonate) film and its application in polymer optoelectronic devices. Adv. Funct. Mater. **15**, 203–208 (2005)
55. Y.-K. Han, M.-Y. Chang, W.-Y. Huang, H.-Y. Pan, K.-S. Ho, T.-H. Hsieh, S.-Y. Pan, Improved performance of polymer solar cells featuring one-dimensional PEDOT nanorods in a modified buffer layer. J. Electrochem. Soc. **158**, K88 (2011)
56. W. Tress, A. Petrich, M. Hummert, M. Hein, K. Leo, M. Riede, Imbalanced mobilities causing S-shaped IV curves in planar heterojunction organic solar cells. Appl. Phys. Lett. **98**, 63301 (2011)
57. A. Kumar, S. Sista, Y. Yang, Dipole induced anomalous S-shape I-V curves in polymer solar cells. J. Appl. Phys. **105**, 94512 (2009)
58. J.C. Wang, X.C. Ren, S.Q. Shi, C.W. Leung, P.K.L. Chan, Charge accumulation induced S-shape J–V curves in bilayer heterojunction organic solar cells. Org. Electron. **12**, 880–885 (2011)
59. W. Tress, K. Leo, M. Riede, Influence of hole-transport layers and donor materials on open-circuit voltage and shape of I–V curves of organic solar cells. Adv. Funct. Mater. **21**, 2140–2149 (2011)
60. W. Tress, S. Corvers, K. Leo, M. Riede, Investigation of driving forces for charge extraction in organic solar cells: transient photocurrent measurements on solar cells showing S-shaped current–voltage characteristics. Adv. Energy Mater. **3**, 873–880 (2013)
61. M. Zhang, H. Wang, C.W. Tang, Hole-transport limited S-shaped I-V curves in planar heterojunction organic photovoltaic cells. Appl. Phys. Lett. **99**, 213506 (2011)